Development of novel anticancer agents for protein targets

Estrada Ortiz, Natalia

CHAPTER 6

GOLD(I) COMPLEXES WITH LANSOPRAZOLE-TYPE LIGANDS: EX VIVO TOXICOLOGICAL EVALUATION

N. Estrada-Ortiz,[a] E. Lopez-Gonzales,[a] E. Post, I. A. M.[a] de Graaf,[a] G. M. M. Groothuis,[a] A. Casini[a,b*]

[a] *Dept. Pharmacokinetics, Toxicology and Targeting, Groningen Research Institute of Pharmacy. University of Groningen. A. Deusinglaan 1, 9713AV Groningen, The Netherlands.*
[b] *School of Chemistry. Cardiff University. Main Building, Park Place, CF103AT Cardiff, United Kingdom.*

Manuscript in preparation

ABSTRACT

In previous studies, bifunctional metallocompounds were synthetized and characterized, to target specifically tumor cells and act as chimeric compounds combining the cytotoxicity of gold and a lansoprazole moiety, which decreases the acidic microenvironment in cancer tissue, thereby increasing the efficacy of the basic drugs. The cytotoxic activity of the compounds was evaluated previously in a small panel of cancer cells, including cell lines sensitive and resistant to cisplatin, and a non-cancerous cell line. These series of compounds showed to be more cytotoxic to the cancer cell lines than in the non-cancerous cell line, suggesting a potential selectivity towards cancer cells. In the present study, the potential selectivity of these compounds was studied in an ex-vivo model, using rat precision cut kidney and liver slices (PCKS and PCLS), to determine to which extent these compounds are toxic to healthy tissue. The results obtained showed a different toxicity profile for the tested compounds, but the stress responses seem to be similar for both evaluated organs. The obtained results open new perspectives towards the design of bifunctional gold complexes for chemotherapeutic applications with reduced toxicity in healthy tissues.

INTRODUCTION

In the drug development process in addition to animal experiments the prediction of toxicity in human tissue and organs is crucial to anticipate possible side effects before starting clinical trials of potential drug-like compounds. 2-D models are by far the most commonly used models to predict effectivity and toxicity for humans. The advantage of these models is the variety of cell types available to study, including primary cells, cell lines, stem cells and cancer cells among others. The main disadvantage is the absence of the complexity of a tissue, with its multitude of cell types playing different roles and secreting different signaling molecules, and the absence of a proper extra cellular matrix to maintain and regulate the function and activities of the specific tissue.[1] Therefore animal models are widely used, where the complexity of a whole organism is intact. However, the use of animals for preclinical studies expose two important problems: the large number of animals used is an ethical problem and the translation of such studies from any species (even primates) to the human situation is not always accurate and presents a risk to the patients entering to the first rounds of clinical trials.[2–5]

However, in 1923 Otto Warburg and later in 1933 HA Krebs used liver tissue slices. They were produced manually, leading to reduced viability and reproducibility.[6,7] After the introduction of the Krumdieck slicer, the tissue slices technique was greatly improved, offering the opportunity to produce slices with precise thickness and sufficiently thin to allow oxygen and substrate supply to all cell layers.[8] The technique is known as precision cut tissue slices (PCTS) and it became a powerful technique, which can be applied to many organs. PCTS contain all cell types of the tissue in their natural environment, with intercellular and cell-matrix interactions remaining intact, making the technic a powerful *in vitro* tool to serve as a model for human diseases, such as fibrosis and cirrhosis. Additionally, the PCTS technique offers the opportunity to test the activity, metabolism, transport and toxicity of new drug candidates, including comparison among species and organs.[6,9–15] PCTS is an FDA-approved model for drug toxicity and metabolism studies and offers an opportunity of reducing the number of animals used in pre-clinical studies.[6,9,16]

In a previous study, Au(I) compounds with ligands were synthetized (Figure 1), featuring lansoprazole as ligand, and studied for their anticancer effects in human cancer cells *in vitro*.[17] Lansoprazole is a drug currently in use for the treatment of ulcers and gastroesophageal reflux disease.[18,19] The clinical efficacy of lansoprazole has been studied in the treatment of duodenal and gastric ulcers, reflux oesophagitis, and eradication of *H. pylori* in combination with clarithromycin and amoxicillin.[18] The postulated mechanism of action is to selectively inhibit the membrane enzyme H^+/K^+ATPase in gastric parietal cells. The enzyme H^+/K^+ATPase is a proton pump located in the apical membrane of parietal cells and is responsible for gastric acid secretion. Proton pump inhibitors (PPIs) exert their effects by blocking the translocation of H^+ to form HCl. Thus, lansoprazole prevents acid formation in the stomach.[18,20]

It has been proposed that PPIs, such as lansoprazole, can modify the acidic microenvironment present in most solid tumors and help to sensitize them to cytotoxic anticancer drugs.[21–24] In tumors the low extracellular pH is a major cause of tumor unresponsiveness to most of the cytotoxic drugs; the H^+ rich tumor microenvironment leads to protonation of the therapeutic agent causing its neutralization and stopping the compound to reach its targets inside the cells.[19,25–28] Within this context, in the last decade, several studies have shown a potential application in cancer research, using proton pump

inhibitors to revert chemoresistance and increase chemosensitivity of different human tumor cells in combination with other cytotoxic drugs.[17,28] Furthermore, lansoprazole and derivatives showed antituberculosis activity targeting cytochrome bc1 and displayed activity against different strains of the mycobacterium.[29]

The structure of lansoprazole includes a benzimidazole ring and a pyridine ring connected through a sulfinyl linkage. The compound is relatively unstable and can be modified in enzymatic and non-enzymatic reactions.[29,30] The compound's metabolic activation occurs by protonation of the nitrogens on both sides of the sulfinyl group. The protonation on the benzimidazole ring causes rearrangement of the sulfinyl into a sulfenic acid or a sulfonamide. The latter can react with two cysteine residues of the H^+K^+-ATPase to form one or two disulfide bonds, which results in complete inhibition of basal and induced acid secretion when two inhibitors are bound per molecule of enzyme.[18,20]

Based on preliminary promising results in our group on the possible application of the Au(I)-lansoprazole derivatives (Figure 1) as potential cytotoxic agents [17] (Table 1) or as antibiotics (data not shown), we decided to investigate the toxicity in healthy tissue, using rat PCTS of liver and kidney. These studies are useful to be able to propose the compounds as good drug candidates for further preclinical investigation.

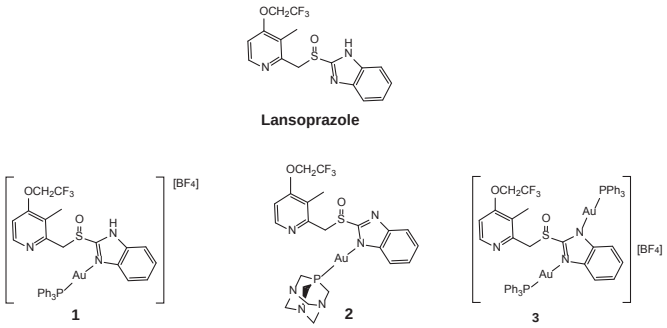

Figure 1. Lansoprazole and derivatives evaluated in this study.

Recently, we have used PCTS to study the toxic effects of experimental anticancer organometallic compounds,[31–34] aminoferrocene-containing pro-drugs,[35] ruthenium-based kinase inhibitors,[36] as well as supramolecular metallocages as possible drug delivery systems.[37] Thus, we report here the use of this methodology to investigate the possible toxic effects of the above mentioned Au(I) lansoprazole derivatives. Specifically, assessment of the ATP content and histomorphological studies were conducted on PCTS from rat liver and kidney treated with the Au(I) compounds in comparison to lansoprazole. Finally, to get more insights about the possible mechanism of the toxicological action, the mRNA expression of specific stress markers was assessed in slices, including expression of genes coding for proteins that play important roles in the pathways of oxidative stress, apoptosis and hypoxia.

RESULTS AND DISCUSSION

VIABILITY AND TC_{50} DETERMINATION

Complexes **1-3** were tested for their possible toxicity in healthy rat kidney and liver PCTS.[6,9] Kidney and liver slices were incubated with various concentrations of each gold complex and after 24 h the viability of the tissues was determined measuring the ATP content (Figure 2). Lansoprazole, cisplatin and auranofin were also tested for comparison.

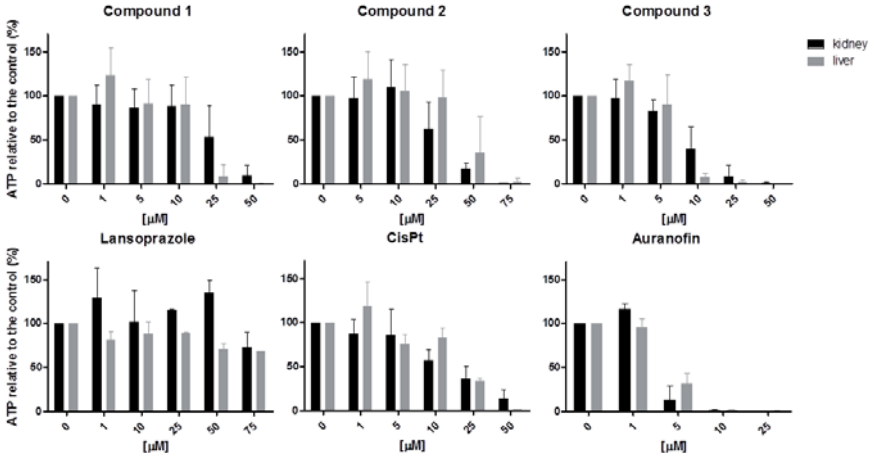

Figure 2. Viability of rat PCKS and PCLS relative to the controls (untreated slices) after treatment with compounds **1-3**, lanzoprazole, cisplatin and auranofin for 24 h. The error bars show the standard deviation of at least three independent experiments.

All the evaluated compounds, including cisplatin and auranofin, displayed a concentration dependent toxicity profile, with complex **3** and auranofin as the most toxic, with TC_{50} below 10 μM. The results obtained in this ex vivo model were compared with the cytotoxicity observed towards the cancer cells (Table 1). For compounds **2** and **3** the safety margin for toxicity was poor with a ratio of TC_{50} PCKS/IC_{50} cells between 1.7 and 4.1. Whereas, for compound **1** the TC_{50} PCKS/IC_{50} cells ratio cells was 20 for kidney slices and 8.9 for liver slices indicating selective toxicity towards cancer cells compared to healthy tissue. Notably, no significant differences were found between toxicity of **2** and **3** compounds in kidney and liver slices.

Table 1. Toxicity of Au(I) complexes in PCKS and PCLS (TC_{50} values) and their comparison with the IC_{50} of the antiproliferative effects in cancer cell lines.

Compound	IC_{50}[a] (μM)		IC_{50} (μM) (average)	TC_{50}[a] (μM)		TC50/IC50	
	A2780	A2780R		kidney	liver	kidney	liver
1	1.1 ± 0.3	0.7 ± 0.1	0.9	18 ± 2	8 ± 3	20	8.9
2	16.2 ± 1.1	13.2 ±4 .6	14.7	27 ± 5	25 ± 3	1.8	1.7
3	1.5±0.3	0.9±0.4	1.2	5 ± 2	4 ± 1	4.1	3.3
Lansoprazole	45.6 ± 2.6	59.0 ± 15.2	52.3	> 50	> 50	0.9	0.9
Cisplatin	2.4 ± 0.6	35.0 ± 7.0	18.7	16 ± 1	24 ± 1	0.9	1.3
Auranofin	ND	ND	NA	2.9 ± 1	4 ± 1	ND	ND

[a] The reported values are the mean ± SD of at least three independent experiments.
ND: Not determined

HISTOMORPHOLOGY

In order to confirm the decrease in viability observed by ATP, further morphological analysis of the PCTS was performed. The characteristic toxic effects on kidney and liver slices of the compounds **1**-**3**, cisplatin and auranofin were evaluated at a concentration close to the calculated TC_{50} for each compound (25 µM for compounds **1**, **2** and cisplatin; 10 µM for compound **3** and 5 µM for auranofin). Periodic acid-Schiff staining (PAS) was used to evaluate kidney slices integrity and particularly to visualize the basement membranes and epithelial brush border in the proximal tubule cells, as reported in the experimental section. Furthermore, haematoxylin and eosin staining was used to visualize the integrity of the hepatocytes present in the liver slices. After 24 h incubation, the untreated kidney slices show minor morphological changes, indicated by pyknosis and swelling of some of the tubular cells (Figure 3A). Pronounced toxic effects were observed upon treatment with complexes **1**, **2** and **3,** which induced dilatation of Bowman's space in the glomerulus and necrosis of the distal tubule cells, as well as discontinuation of the brush border in some of the proximal tubule cells (Figure 3B, 3C and 3D). In contrast, exposure of slices to cisplatin (Figure 3E) showed injury to the proximal tubular cells with loss of nuclei and more distinct damage of the brush border; additionally, damage of the distal tubule is evident as previously reported in the literature.[11] Interestingly, the morphological characteristics of the samples treated with auranofin present similar damaged as the evaluated Au complexes, with a more pronounced damage to the distal tubular cells. In the case of liver slices, after 24 h incubation, the hepatocytes present normal large nuclei and defined shape (Figure 4A) that are indicative of healthy tissue. However, the morphological changes observed in liver slices exposed to the evaluated compounds showed similar toxic effect of compounds **1** and **3** (figure 4B and 4D), with evidence of pyknosis, necrosis and loss of nuclei. However, complex **2** seems to induce slightly less toxicity at the morphological level (Figure 4C) showing some pyknosis and necrosis, but occasional viable cells are observed. Liver slices treated with cisplatin and auranofin showed extensive damage, and pyknosis and necrosis were induced by all tested metal complexes (Figure 4E and 4F). The tested concentrations were too high to observe differential damage in different cell types. Currently, more experiments are in progress using concentrations around the TC_{25} value for each compound.

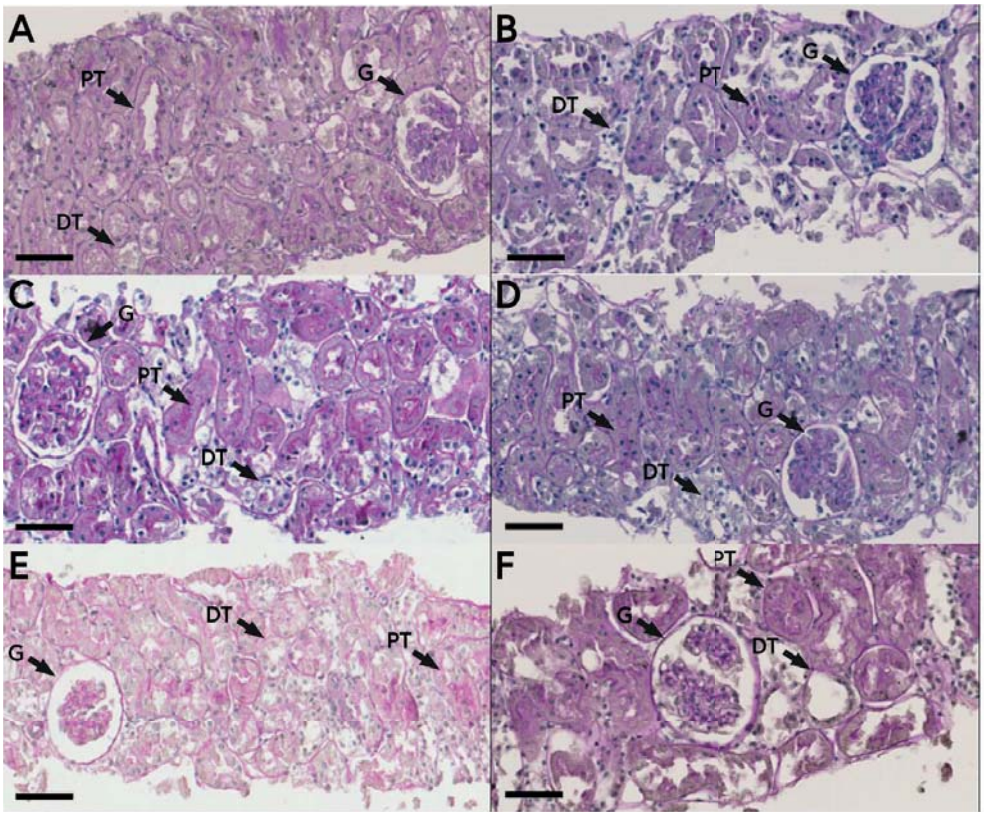

Figure 3. Morphology of rat kidney slices. A: 24 h control incubation; B: compound **1** (25 μM); C: compound **2** (25 μM); D: compound **3** (10 μM); E: cisplatin (25 μM) and F: auranofin (5 μM). PT: proximal tubule, DT: distal tubule, G: glomerulus. Scale bar indicates 50 μm.

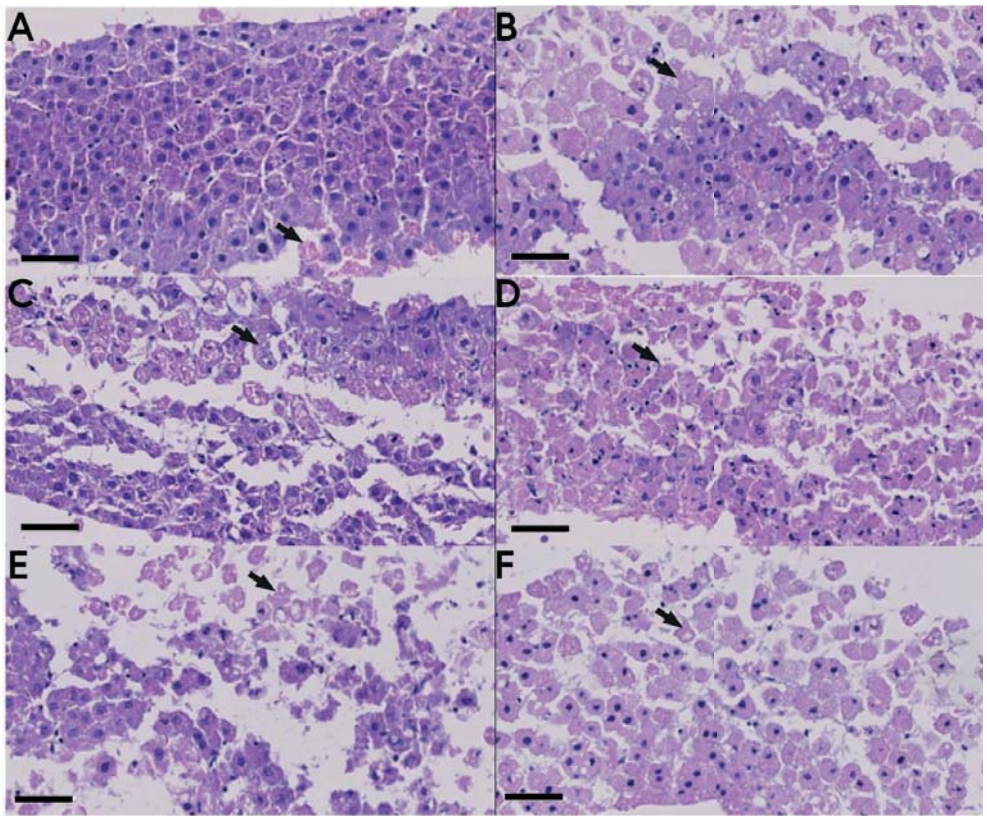

Figure 4. Morphology of rat liver slices. A: 24 h control incubation; B: compound **1** (25 µM); C: compound **2** (25 µM); D: compound **3** (10 µM); E: cisplatin (25 µM) and F: auranofin (5 µM). Arrows indicate necrotic cells. Scale bar indicates 50 µm.

DETERMINATION OF STRESS MARKERS EXPRESSION

To get insights of the specific type of stress that the Au complexes evaluated in this study, we selected specific genes that code for proteins that belong to pathways that are activated under hypoxia (Hif1a),[38] oxidative stress (Nrf2)[39] and DNA damage (p53)[40]. Based on the work of Limonciel, et al., 2015,[41] we chose two or three genes related with the mentioned pathways that displayed significant up or down regulation after treating human and rat hepatocytes, and RPTEC/TERT1 cells (human renal proximal tubule cell line transfected with human telomerase) with several known toxicants.[41] All the selected bio-markers are expressed by kidney and liver cells. Thus, liver and kidney slices were treated with the compounds at concentrations below and close to the calculated TC_{50} values (1 and 10 µM for compound **1** and **3,** 5 and 25 µM for compound **2**, 50 and 75 µM for lansoprazole) during 24 h.

From the Hif1α (hypoxia-inducible factor 1 α) pathway, we selected to measure the expression levels of ALDOA that codes for the Fructose-Bisphosphate Aldolase A enzyme, ENO2 that codes for enolase 2 and SLC2A1 that codes for the glucose transporter protein type 1 (GLUT1). All these genes promote survival of the cells in hypoxic conditions by inducing glycolysis. In the case of PCKS significant up or down regulation of any of the selected genes was not observed (Figure 5), indicating that the compounds do not promote a hypoxic environment as a toxicity mechanism. In the case of PCLS, the

responses are more diverse, where exposure of PCLS to compound **1** seems to induce an upregulation of SLC2A1 gene at the highest concentration only. Moreover, treatment with compound **3** at 10 µM induces upregulation about 3-fold of ENO2 compared with the untreated samples. These results suggest some activation of the hypoxia pathway in the liver slices. Lansoprazole did not induce any change in the expression of the tested genes. More experiments are needed to fully understand if hypoxia is the toxicity mechanism specifically in the case of liver tissue using more bio-markers that are modulated in response to hypoxia, such as Hif1α and FABP3 (fatty acid binding protein 3).

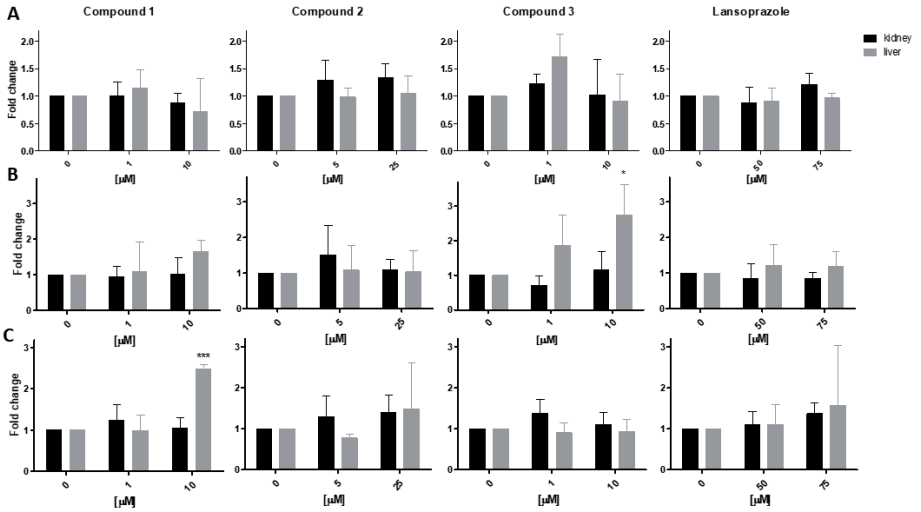

Figure 5. Gene expression of ALDOA (**A**), ENO2 (**B**) and SLC2A1 (**C**) in kidney and liver slices exposed to compounds **1**, **2**, **3** and lansoprazole for 24 h, in comparison to untreated slices set as 1. The error bars show the standard deviation of at least three independent experiments.

The selected genes from the Nrf2 pathway include GCLM and HMOX-1. GCLM codes for Glutamate-Cysteine Ligase Modifier Subunit, part of the Glutamate-cysteine ligase and is the first enzyme of the glutathione biosynthetic pathway. HMOX-1 codes for Heme Oxygenase 1 which is an essential enzyme in heme catabolism and plays an important role as antioxidant under oxidative stress conditions. Both genes are over expressed under oxidative stress conditions in kidney and liver tissue to compensate the excessive production of free radicals.[42–44] GLCM expression is significantly upregulated by the higher concentration of compound **3** in kidney slices, whereas in liver slices the effect is not evident. HMOX-1 expression is significantly upregulated by the higher concentration of compound **3** in kidney and liver slices. HMOX-1 displays a trend towards upregulation after treatment of PCKS and PCLS with compounds **1** and **2**, even though the differences are not significant in all the cases, an analysis of individual experiments revealed a clear trend to upregulation of both genes (Figure 6). Lansoprazole did not induce any change in the expression of the tested genes. These findings suggest oxidative stress as the possible mechanism of toxicity in kidney and liver slices being more pronounced in kidney. More experiments evaluating the glutathione and thioredoxin redox balance assays, could lead to confirmation of our findings

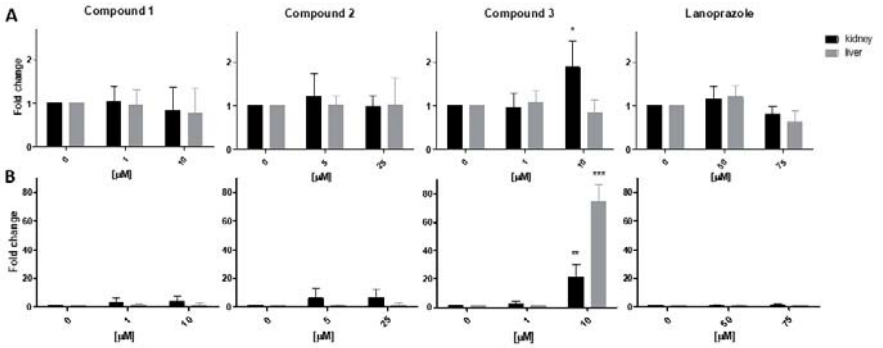

Figure 6. Gene expression of GCLM (**A**) and HMOX-1 (**B**) in kidney and liver slices exposed to compounds **1**, **2**, **3** and lansoprazole for 24 h, in comparison to untreated slices set as 1. The error bars show the standard deviation of at least three independent experiments.

The p53 pathway was explored by determining the expression levels of protein p53 that stimulates the expression of a set of downstream target genes that can induce apoptosis, facilitate DNA repair or activate cell cycle arrest upon cellular stress signals induced by DNA damage, oncogene activation and hypoxia.[45–48] BAX that codes for the Bcl-2-associated X protein that plays an important role in apoptosis.[49] Additionally SULF-2 gene was evaluated, it codes for sulfatase 2 enzyme, which is upregulated upon activation of p53 due to DNA damage, thereby affecting the cell cycle.[50] Neither p53, BAX or SULF-2 showed major regulation changes upon treatment of kidney and liver slices (Figure 7). These findings are in line with results obtained to assess the caspase 3 and 7 activation in PCKS (results not shown), where after treatment with the compounds no evidence of caspase activation was found, indicating that apoptosis is not the mechanism of cell death in these tissue slices.

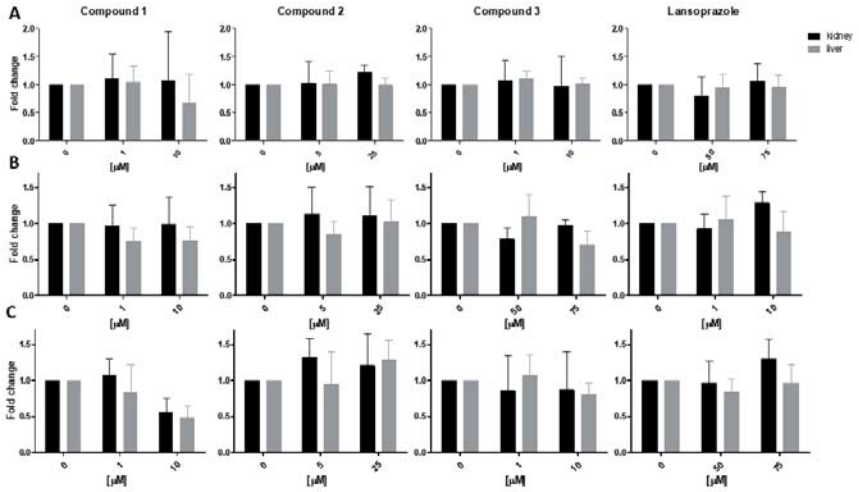

Figure 7. Gene expression of p53 (**A**), BAX (**B**) and SULF-2 (**C**) in kidney and liver slices exposed to compounds **1**, **2**, **3** and lansoprazole for 24 h, in comparison to untreated slices set as 1. The error bars show the standard deviation of at least three independent experiments.

CONCLUSIONS

The potential therapeutic application of lansoprazole Au(I) derivatives with antiproliferative effect[17] and as antituberculosis agents, prompted us to study the toxicity in healthy tissue using kidney and liver slices aiming to get insights about the possible side effects if the compounds are administered in vivo. We assessed the toxicity by ATP content and histomorphology in PCKS and PCLS. Additionally, mRNA expression of specific stress markers was assessed in slices, including expression of genes coding for proteins that play important roles in pathways of oxidative stress, apoptosis and hypoxia.

The obtained ATP results showed a different toxicity profile for the tested compounds. Compound **2** shows the lowest toxicity in both liver and kidney slices, also lower than cisplatin, whereas compounds **1** and **3** are more toxic in the liver slices. Notably, both compounds bear phosphine ligands, known to be an intrinsically toxic ligand**.** However, in kidney slices compound **1** is less toxic than compound **3**, and is equal to compound **2.** Compound **3** is the most toxic in both organs. The presence of a second Au(I) center in **3**, may be responsible for the higher toxicity in healthy tissue compared to **1** and **2**.

However, not the intrinsic toxicity but the selectivity of toxicity in healthy organs versus cancer cells is the most relevant parameter. This is estimated by calculating the ratio of the TC_{50} in slices to the IC_{50} in the cancer cells. Using this ratio as the potential selectivity of the complexes, compound **1** presents the best ratio of toxicity in healthy tissue to anticancer efficacy, which is much higher than that for cisplatin, which may indicate that this compound can lead to a better drug candidate for further development. However, it should be stressed that these ratios do not represent the absolute values of selectivity, because the experimental methods in cell lines and in slices are different. For instance, the slices are incubated for 24 h and the cancer cells are investigated after 72 h. Moreover, the medium composition is different, and the potential effect of protein binding could be very different in the two systems. Nevertheless, the calculated ratios can be used to compare the different compounds with standard drugs like cisplatin. In vivo animal experiments or experiments with healthy tissue slices and tumor tissue slices, preferably from human origin, could give a better estimation of the selectivity of the drugs for the cancer cells.

Notably, the histomorphology evaluation shows similarities for all three Au(I) complexes with respect to the specific kidney cell types that suffer the most extensive damage, where they seem to have a preferent toxicity towards the distal tubular cells. In contrast to cisplatin which is known to show toxicity in the proximal tubular cells as described in previous reports.[11,34] Regarding the liver histomorphological evaluation, all the tested compounds including cisplatin and auranofin induce extensive hepatocellular necrosis.

Interestingly, of all the stress pathways evaluated, the clearest impact was on the Nrf2 pathway, indicating oxidative stress as a possible mechanism of toxicity. This result is in line with the previously reported data, which showed the effects of Au(I) complexes on the inhibition of the seleno-enzyme thioredoxin reductase (TrxR) involved in the maintenance of the intracellular redox balance.[51,52] For future studies, it might be relevant to include specific markers for distinct cell types in the kidney and the liver to get more information about the cell-specific toxicity of the compounds evaluated in this study.

The broad spectrum of applications of the PCTS technology allows us to study in detail the mechanism of the toxicity of the potential drug candidates, using a reduced number of animals with minimal suffering. Using PCTS it is possible to obtain valuable knowledge on the structure-toxicity relationship of experimental compounds, enabling further optimization and selection of better candidates with improved properties and reduced toxicity in healthy tissue.

The obtained results open new perspectives towards the understanding of the selectivity and mechanism of toxicity of the evaluated chimeric compounds and prompt us to continue with the design of more families of bifunctional gold complexes for medical applications and diverse targets with reduced toxicity in healthy tissues.

EXPERIMENTAL SECTION

PREPARATION OF RAT PRECISION-CUT LIVER AND KIDNEY SLICES (PCLS-PCKS)

Male Wistar rats (Charles River, France) of 250-300 g were housed under a 12 h dark/light cycle at constant humidity and temperature. Animals were permitted *ad libitum* access to tap water and standard lab chow. All experiments were approved by the committee for care and use of laboratory animals of the University of Groningen and were performed according to strict governmental and international guidelines.

Kidneys were harvested (from rats anesthetized with isoflurane) and immediately placed in University of Wisconsin solution (UW, ViaSpan, 4ºC) until further use. After removing fat, kidneys were cut in half lengthwise using a scalpel, and cortex cores of 5 mm diameter were made from each half perpendicular to the cut surface using disposable Biopsy Punches (KAI medical, Japan). PCKS were made as described by de Graaf et al.[6,9] The cores were sliced with a Krumdieck tissue slicer (Alabama R&D, Munford, AL, USA) in ice-cold Krebs-Henseleit buffer, pH 7.4 saturated with carbogen (95% O_2 and 5% CO_2). Liver slices (5 mg, ~250 µm thickness) and kidney slices (3 mg, ~150 µm thickness), were incubated individually in 12-well plates (Greiner bio-one GmbH, Frickenhausen, Austria), at 37°C in 1.3 mL Williams' medium E (WME, Gibco by Life Technologies, UK) with glutamax-1, supplemented with 25 mM D-glucose (Gibco) and streptomycin(Gibco) (PCLS) ciprofloxacin HCl (PCKS) (10 µg/mL, Sigma-Aldrich, Steinheim, Germany) in an incubator (Panasonic biomedical) in an atmosphere of 80% O_2 and 5% CO_2 with shaking (90 times/min). Slices were pre-incubated 1 h and then transferred to plates with fresh medium with the tested compounds to remove debris and dead cells. Stock solutions of compounds **1** to **3,** auranofin were prepared by diluting a stock solution (10^{-2} M in DMSO, ethanol in the case of auranofin; 10^{-3} M in water for cisplatin). The final concentration of DMSO and ethanol during the PCLS and PCKS incubation was always below 1 and 0.025 %, respectively to exclude solvent toxicity. For each concentration, three slices were incubated individually for one hour in WME and subsequently, different dilutions of the compounds were added to the wells, to obtain a final concentration from 1 up to 75 µM. After this, PCKS were incubated for 24 h.

VIABILITY AND TC_{50} DETERMINATION

After the incubation, slices were collected for ATP and protein determination, by snap freezing them in 1 ml of ethanol (70% v/v) containing 2 mM EDTA with pH=10.9. After thawing the slices were homogenized using a mini bead beater and centrifuged. The supernatant was used for the ATP essay and the pellet was dissolved in 5N NaOH for the protein essay. The viability of PCKS was determined by measuring the ATP using the ATP Bioluminescence Assay kit CLS II (Roche, Mannheim, Germany) as

described previously.[9] The ATP content was corrected by the protein amount of each slice and expressed as pmol/µg protein. The protein content of the PCKS was determined by the Bio-Rad DC Protein Assay (Bio-Rad, Munich, Germany) using bovine serum albumin (BSA, Sigma-Aldrich, Steinheim, Germany) for the calibration curve. The TC_{50} value was calculated as the concentration reducing the viability of the slices by 50%, in terms of ATP content corrected by the protein amount of each slice and relative to the slices without any treatment using a nonlinear fitting of log(concentration compound) vs response and is presented as a mean (± SD) of at least three independent experiments.

HISTOMORPHOLOGY

After incubation, liver and kidney slices were fixated in 4% formalin for 24 hours and stored in 70% ethanol at 4°C until processing for morphology studies. After dehydration, the slices were embedded in paraffin and 4 µm sections were made, which were mounted on glass slides and H&E and PAS staining was used for histopathological evaluation. Afterwards, the glass slides were deparaffinised with xylene and ethanol 100%. For the H&E staining the glass slides were hydrated in 50% ethanol, followed by hematoxylin staining for 5 minutes, then rinsed with tap water and treated with acid and basic solutions of ethanol, later the glass slides were stained with eosin for 2 minutes and washed with ethanol 100% and xylene. For the PAS staining the glass slides were washed with distilled water, followed by treatment with a 1% aqueous solution of periodic acid for 20 minutes and Schiff reagent for 20 minutes, the slides were rinsed with tap water, finally, a counterstain with Mayer's hematoxylin for 5 minutes was used to visualize the nuclei.

DETERMINATION OF STRESS MARKERS EXPRESSION

RNA isolation

Three precision cut kidney slices from each treatment group were snap-frozen in RNase free Eppendorf's. RNA was isolated with the Maxwell® 16 simplyRNA Tissue Kit (Promega, Leiden, the Netherlands). Slices were homogenised in homogenisation buffer using a minibead beater. The homogenate was diluted 1:1 with lysis buffer. The mixture was processed according to the manufacturer's protocol using the Maxwell machine. RNA concentration was quantified on a NanoDrop One UV-Vis Spectrophotometer (Thermoscientific, Wilmington, US) right before conversion to cDNA.

cDNA generation

RNA samples were diluted to 0,5 µg in 8,5 µl of RNAsa free water. cDNA was generated from RNA using random primers with TaqMan Reverse Transcription Reagents Kits (Applied Biosystems, Foster City, CA). To each sample the following solutions were added: 2,5 µL 5x RT-buffer, 0,25 µL 10mM dNTP's, 0,25 µL Rnasin (10 units), 0,5 µL M-MLV Reverse Transcriptase (100 units), 0,5 µL random primers. cDNA was generated in the Eppendorf mastercycler (Hamburg, Germany) with a gradient of 20°C for 10 min, 42°C for 30 min, 20°C for 12 min, 99°C for 5 min and finally, 20°C for 5 min.

qPCR

Real-time quantitative PCR was used to determine relative mRNA levels of a set of specific genes involved in toxicity pathways. PCR Was performed using SensiMixTM SYBR Low-ROX kit (Bioline, London, UK) with the QuantStudio 7 Flex Real-Time PCR System (Thermoscientific, Wilmington, US) with 1 cycle of 10 min at 95°C, 40 cycles of 15 sec at 95°C and 25 sec at 60°C, with a final dissociation stage of 15 sec at 95°C, 1 min at 60°C and 15 sec at 95°C. cDNA for each sample was diluted to 10 ng/µ

l and measured in triplicate. All primers were purchased from Sigma-Aldrich. Fold induction of each gene was calculated using the housekeeping gene GAPDH.

Primer sequences used in qPCR:

ALDOA: 5′-ACGAGGTTCTGGTGACCCTA′-3 (forward), 5′-CCGGAGCTACAATTCGGTGA-3′ (reverse);
ENO2: 5′-GTACCACACACTCAAGGGGG′-3 (forward), 5′-TCGTATTTGCCATCGCGGTA-3′ (reverse);
SLC2A1: 5′-TCAAACATGGAACCACCGCT′-3 (forward), 5′-AGAAACCCATAAGCACGGCA-3′ (reverse);
GCLM: 5′-TCAAGCTCACAACTCAGGGG′-3 (forward), 5′-CGCCAGGGAGGTACTCAAAC-3′ (reverse);
HMOX-1: 5′-CACGCATATACCCGCTACCT′-3 (forward), 5′-AAGGCGGTCTTAGCCTCTTC-3′ (reverse);
p53: 5′- CCCCTGAAGACTGGATAAC-3′ (forward), and 5′-AACTCTGCAACATCCTGGGG-3′ (reverse);
BAX: 5′-ACAGGGGCCTTTTTGTTACAG-3′ (forward), 5′-GGGGAGTCCGTGTCCACGTCA-3′ (reverse);
SULF2: 5′-CGTGTGTGTTTAGAGGCGAGC′-3 (forward), 5′-AGCCTCTTTCCGCTTTTTGGT-3′ (reverse);
GAPDH: 5′-CGCTGGTGCTGAGTATGTCG′-3 (forward), 5′-CTGTGGTCATGAGCCCTTCC-3′ (reverse).

STATISTICS

A minimum of three independent experiments were performed using slices in triplicates from each rat kidney or liver. Statistical testing was performed with one-way ANOVA with each individual experiment as random effect. We performed a Tukey HSD post-hoc test for pairwise comparisons. A p-value of ≤ 0.05 was considered to be significant. In all graphs and tables the mean values and standard deviation (SD) are shown.

REFERENCES

(1) Imamura, Y.; Mukohara, T.; Shimono, Y.; Funakoshi, Y.; Chayahara, N.; Toyoda, M.; Kiyota, N.; Takao, S.; Kono, S.; Nakatsura, T.; Minami, H. Comparison of 2D- and 3D-Culture Models as Drug-Testing Platforms in Breast Cancer. *Oncol. Rep.* **2015**, *33* (4), 1837–1843.

(2) Ahuja, V.; Bokan, S.; Sharma, S. Predicting Toxicities in Humans by Nonclinical Safety Testing: An Update with Particular Reference to Anticancer Compounds. *Drug Discov. Today* **2017**, *22* (1), 127–132.

(3) Attarwala, H. TGN1412: From Discovery to Disaster. *J. Young Pharm. JYP* **2010**, *2* (3), 332–336.

(4) Butler, D.; Callaway, E. Scientists in the Dark after French Clinical Trial Proves Fatal. *Nat. News* **2016**, *529* (7586), 263.

(5) Kimmelman, J.; Federico, C. Consider Drug Efficacy before First-in-Human Trials. *Nat. News* **2017**, *542* (7639), 25.

(6) de Graaf, I. A. M.; Groothuis, G. M.; Olinga, P. Precision-Cut Tissue Slices as a Tool to Predict Metabolism of Novel Drugs. *Expert Opin. Drug Metab. Toxicol.* **2007**, *3* (6), 879–898.

(7) Olinga, P.; Meijer, D. K. F.; Slooff, M. J. H.; Groothuis, G. M. M. Liver Slices in in Vitro Pharmacotoxicology with Special Reference to the Use of Human Liver Tissue. *Toxicol. In Vitro* **1997**, *12* (1), 77–100.

(8) Krumdieck, C. L.; dos Santos, J.; Ho, K.-J. A New Instrument for the Rapid Preparation of Tissue Slices. *Anal. Biochem.* **1980**, *104* (1), 118–123.

(9) de Graaf, I. A. M.; Olinga, P.; de Jager, M. H.; Merema, M. T.; de Kanter, R.; van de Kerkhof, E. G.; Groothuis, G. M. M. Preparation and Incubation of Precision-Cut Liver and Intestinal Slices for Application in Drug Metabolism and Toxicity Studies. *Nat. Protoc.* **2010**, *5* (9), 1540–1551.

(10) Parrish, A. R.; Gandolfi, A. J.; Brendel, K. Precision-Cut Tissue Slices: Applications in Pharmacology and Toxicology. *Life Sci.* **1995**, *57* (21), 1887–1901.

(11) Vickers, A. E. M.; Rose, K.; Fisher, R.; Saulnier, M.; Sahota, P.; Bentley, P. Kidney Slices of Human and Rat to Characterize Cisplatin-Induced Injury on Cellular Pathways and Morphology. *Toxicol. Pathol.* **2004**, *32* (5), 577–590.
(12) Olinga, P.; Schuppan, D. Precision-Cut Liver Slices: A Tool to Model the Liver Ex Vivo. *J. Hepatol.* **2013**, *58* (6), 1252–1253.
(13) Vickers, A. E. M.; Fisher, R. L. Evaluation of Drug-Induced Injury and Human Response in Precision-Cut Tissue Slices. *Xenobiotica Fate Foreign Compd. Biol. Syst.* **2013**, *43* (1), 29–40.
(14) Wolf, A.; Vickers, A.; Olinga, P.; Braun, A.; Martin, C.; Groothuis, G.; Shangari, N. Precision-Cut Tissue Slices Revisited. *Toxicol. Suppl. Toxicol. Sci.* **2011**, *120* (Supplement 2), 379–379.
(15) Poosti, F.; Pham, B. T.; Oosterhuis, D.; Poelstra, K.; Goor, H. van; Olinga, P.; Hillebrands, J.-L. Precision-Cut Kidney Slices (PCKS) to Study Development of Renal Fibrosis and Efficacy of Drug Targeting Ex Vivo. *Dis. Model. Mech.* **2015**, *8* (10), 1227–1236.
(16) Groothuis, G. M. M.; Casini, A.; Meurs, H.; Olinga, P. Chapter 3:Translational Research in Pharmacology and Toxicology Using Precision-Cut Tissue Slices. In *Human-based Systems for Translational Research*; 2014; pp 38–65.
(17) Serratice, M.; Bertrand, B.; Janssen, E. F. J.; Hemelt, E.; Zucca, A.; Cocco, F.; Cinellu, M. A.; Casini, A. Gold(I) Compounds with Lansoprazole-Type Ligands: Synthesis, Characterization and Anticancer Properties in Vitro. *MedChemComm* **2014**, *5* (9), 1418–1422.
(18) Gremse, D. A. Lansoprazole: Pharmacokinetics, Pharmacodynamics and Clinical Uses. *Expert Opin. Pharmacother.* **2001**, *2* (10), 1663–1670.
(19) Miyashita, T.; Shah, F. A.; Harmon, J. W.; Marti, G. P.; Matsui, D.; Okamoto, K.; Makino, I.; Hayashi, H.; Oyama, K.; Nakagawara, H.; Tajima, H.; Fujita, H.; Takamura, H.; Murakami, M.; Ninomiya, I.; Kitagawa, H.; Fushida, S.; Fujimura, T.; Ohta, T. Do Proton Pump Inhibitors Protect against Cancer Progression in GERD? *Surg. Today* **2013**, *43* (8), 831–837.
(20) Shin, J. M.; Kim, N. Pharmacokinetics and Pharmacodynamics of the Proton Pump Inhibitors. *J Neurogastroenterol Motil* **2013**, *19* (1), 25–35.
(21) Barar, J.; Omidi, Y. Dysregulated PH in Tumor Microenvironment Checkmates Cancer Therapy. *BioImpacts BI* **2013**, *3* (4), 149–162.
(22) Spugnini, E.; Fais, S. Proton Pump Inhibition and Cancer Therapeutics: A Specific Tumor Targeting or It Is a Phenomenon Secondary to a Systemic Buffering? *Semin. Cancer Biol.*
(23) Azzarito, T.; Venturi, G.; Cesolini, A.; Fais, S. Lansoprazole Induces Sensitivity to Suboptimal Doses of Paclitaxel in Human Melanoma. *Cancer Lett.* **2015**, *356* (2, Part B), 697–703.
(24) Yu, M.; Lee, C.; Wang, M.; Tannock, I. F. Influence of the Proton Pump Inhibitor Lansoprazole on Distribution and Activity of Doxorubicin in Solid Tumors. *Cancer Sci.* **2015**, *106* (10), 1438–1447.
(25) Trédan, O.; Galmarini, C. M.; Patel, K.; Tannock, I. F. Drug Resistance and the Solid Tumor Microenvironment. *JNCI J. Natl. Cancer Inst.* **2007**, *99* (19), 1441–1454.
(26) Daniel, C.; Bell, C.; Burton, C.; Harguindey, S.; Reshkin, S. J.; Rauch, C. The Role of Proton Dynamics in the Development and Maintenance of Multidrug Resistance in Cancer. *Biochim. Biophys. Acta BBA - Mol. Basis Dis.* **2013**, *1832* (5), 606–617.
(27) Fais, S. Evidence-Based Support for the Use of Proton Pump Inhibitors in Cancer Therapy. *J. Transl. Med.* **2015**, *13*, 368.
(28) Spugnini, E. P.; Sonveaux, P.; Stock, C.; Perez-Sayans, M.; De Milito, A.; Avnet, S.; Garcìa, A. G.; Harguindey, S.; Fais, S. Proton Channels and Exchangers in Cancer. *Biochim. Biophys. Acta BBA - Biomembr.* **2015**, *1848* (10, Part B), 2715–2726.
(29) Rybniker, J.; Vocat, A.; Sala, C.; Busso, P.; Pojer, F.; Benjak, A.; Cole, S. T. Lansoprazole Is an Antituberculous

Prodrug Targeting Cytochrome Bc1. *Nat. Commun.* **2015**, *6*, 7659.
(30) Pearce, R. E.; Rodrigues, A. D.; Goldstein, J. A.; Parkinson, A. Identification of the Human P450 Enzymes Involved in Lansoprazole Metabolism. *J. Pharmacol. Exp. Ther.* **1996**, *277* (2), 805–816.
(31) Bertrand, B.; Stefan, L.; Pirrotta, M.; Monchaud, D.; Bodio, E.; Richard, P.; Le Gendre, P.; Warmerdam, E.; de Jager, M. H.; Groothuis, G. M. M.; Picquet, M.; Casini, A. Caffeine-Based Gold(I) N-Heterocyclic Carbenes as Possible Anticancer Agents: Synthesis and Biological Properties. *Inorg. Chem.* **2014**, *53* (4), 2296–2303.
(32) Bertrand, B.; Citta, A.; Franken, I. L.; Picquet, M.; Folda, A.; Scalcon, V.; Rigobello, M. P.; Le Gendre, P.; Casini, A.; Bodio, E. Gold(I) NHC-Based Homo- and Heterobimetallic Complexes: Synthesis, Characterization and Evaluation as Potential Anticancer Agents. *J. Biol. Inorg. Chem. JBIC Publ. Soc. Biol. Inorg. Chem.* **2015**, *20* (6), 1005–1020.
(33) Muenzner, J. K.; Rehm, T.; Biersack, B.; Casini, A.; de Graaf, I. A. M.; Worawutputtapong, P.; Noor, A.; Kempe, R.; Brabec, V.; Kasparkova, J.; Schobert, R. Adjusting the DNA Interaction and Anticancer Activity of Pt(II) N-Heterocyclic Carbene Complexes by Steric Shielding of the Trans Leaving Group. *J. Med. Chem.* **2015**, *58* (15), 6283–6292.
(34) Estrada-Ortiz, N.; Guarra, F.; de Graaf, I. A. M.; Marchetti, L.; de Jager, M. H.; Groothuis, G. M. M.; Gabbiani, C.; Casini, A. Anticancer Gold N-Heterocyclic Carbene Complexes: A Comparative in Vitro and Ex Vivo Study. *ChemMedChem* **2017**, *12* (17), 1429–1435.
(35) Daum, S.; Chekhun, V. F.; Todor, I. N.; Lukianova, N. Y.; Shvets, Y. V.; Sellner, L.; Putzker, K.; Lewis, J.; Zenz, T.; de Graaf, I. A. M.; Groothuis, G. M. M.; Casini, A.; Zozulia, O.; Hampel, F.; Mokhir, A. Improved Synthesis of N-Benzylaminoferrocene-Based Prodrugs and Evaluation of Their Toxicity and Antileukemic Activity. *J. Med. Chem.* **2015**, *58* (4), 2015–2024.
(36) Rajaratnam, R.; Martin, E. K.; Dörr, M.; Harms, K.; Casini, A.; Meggers, E. Correlation between the Stereochemistry and Bioactivity in Octahedral Rhodium Prolinato Complexes. *Inorg. Chem.* **2015**, *54* (16), 8111–8120.
(37) Schmidt, A.; Molano, V.; Hollering, M.; Pöthig, A.; Casini, A.; Kühn, F. E. Evaluation of New Palladium Cages as Potential Delivery Systems for the Anticancer Drug Cisplatin. *Chem. Weinh. Bergstr. Ger.* **2016**, *22* (7), 2253–2256.
(38) Semenza, G. L. Hypoxia-Inducible Factor 1 (HIF-1) Pathway. *Sci STKE* **2007**, *2007* (407), cm8-cm8.
(39) Ma, Q. Role of Nrf2 in Oxidative Stress and Toxicity. *Annu. Rev. Pharmacol. Toxicol.* **2013**, *53*, 401–426.
(40) Lane, D. P. P53, Guardian of the Genome. *Nature* **1992**, *358* (6381), 15–16.
(41) Limonciel, A.; Moenks, K.; Stanzel, S.; Truisi, G. L.; Parmentier, C.; Aschauer, L.; Wilmes, A.; Richert, L.; Hewitt, P.; Mueller, S. O.; Lukas, A.; Kopp-Schneider, A.; Leonard, M. O.; Jennings, P. Transcriptomics Hit the Target: Monitoring of Ligand-Activated and Stress Response Pathways for Chemical Testing. *Toxicol. Vitro Int. J. Publ. Assoc. BIBRA* **2015**, *30* (1 Pt A), 7–18.
(42) Cheng, M.-L.; Lu, Y.-F.; Chen, H.; Shen, Z.-Y.; Liu, J. Liver Expression of Nrf2-Related Genes in Different Liver Diseases. *Hepatobiliary Pancreat. Dis. Int. HBPD INT* **2015**, *14* (5), 485–491.
(43) Zalups, R. K.; Koropatnick, D. J. *Cellular and Molecular Biology of Metals*; CRC Press, 2010.
(44) Nath, K. A.; Grande, J. P.; Haggard, J. J.; Croatt, A. J.; Katusic, Z. S.; Solovey, A.; Hebbel, R. P. Oxidative Stress and Induction of Heme Oxygenase-1 in the Kidney in Sickle Cell Disease. *Am. J. Pathol.* **2001**, *158* (3), 893–903.
(45) Vazquez, A.; Bond, E. E.; Levine, A. J.; Bond, G. L. The Genetics of the P53